

# Hearing dummies: Individualised computer models of hearing impairment

Manasa R. Panda<sup>1,2</sup>, Wendy Lecluyse<sup>1,3</sup>, Christine M. Tan<sup>1</sup>, Tim Jürgens<sup>1,4</sup>, and Ray Meddis<sup>1</sup>

<sup>1</sup>Department of Psychology, University of Essex, Colchester, UK.

<sup>2</sup>Dept. of Audiology and Speech Language Pathology, Medical College Hospital and Research Center, SRM University, India

<sup>3</sup>School of Applied Social Sciences, University Campus Suffolk, Ipswich, UK

<sup>4</sup>Cluster of Excellence “Hearing4all”, Department of Medical Physics and Acoustics, University of Oldenburg, Germany

Corresponding author:

Wendy Lecluyse

University Campus Suffolk

School of Applied Social Sciences

Waterfront Building

Ipswich, UK

IP4 1QJ

[w.lecluyse@ucs.ac.uk](mailto:w.lecluyse@ucs.ac.uk)

## KEY WORDS

Auditory profiles, auditory model, normal and impaired hearing

## ABBREVIATIONS AND ACRONYMS

AN	auditory nerve
BF	best frequency
BM	basilar membrane
DPOAE	distortion product otoacoustic emission
DRNL	Dual Resonance Nonlinearity
EP	endocochlear potential
$f_m$	masker frequency
$f_t$	probe frequency
IFMC	Iso Forward Masking Contour
IHC	inner hair cell
OHC	outer hair cell
SIUD	single interval up/down procedure
SPL	sound pressure level
TMC	Temporal Masking Curve

## **ABSTRACT**

### **Objective**

Our aim was to explore the usage of individualised computer models to simulate hearing loss based on detailed psychophysical assessment and to offer hypothetical diagnoses of the underlying pathology.

### **Design**

Individualised computer models of normal and impaired hearing were constructed and evaluated using the psychophysical data obtained from human listeners. Computer models of impaired hearing were generated to reflect the hypothesised underlying pathology (e.g. dead regions, outer hair cell dysfunction or reductions in endocochlear potential). These models were evaluated in terms of their ability to replicate the original patient data.

### **Study Sample**

Auditory profiles were measured for 2 normal and 5 hearing impaired listeners using a battery of three psychophysical tests (absolute thresholds, frequency selectivity and compression).

### **Results**

The individualised computer models were found to match the data. Useful fits to the impaired profiles could be obtained by changing only a single parameter in the model of normal hearing. Sometimes, however, it was necessary to include an additional dead region.

### **Conclusion**

The creation of individualised computer models of hearing loss can be used to simulate auditory profiles of impaired listeners and suggest hypotheses concerning the underlying peripheral pathology.

## INTRODUCTION

Computer models of the auditory periphery are increasingly being used to understand the nature of sensorineural hearing loss (Heinz et al, 2001; Bruce et al, 2003; Zilany and Bruce, 2006; Jepsen and Dau, 2011; Meddis et al, 2010). The basic paradigm of these studies is to show how pathological changes to the underlying physiology give rise to changes observed in different types of sensorineural hearing loss. The present paper aims to take this process further and develop procedures for building individualised models that simulate the specific auditory profile of a single patient.

This approach has a number of potential benefits. The first concerns diagnosis. If it is possible to identify the parameters of the model that need to be changed in order to reproduce the patient's auditory profile, we will then have a hypothetical diagnosis of the disease. This is particularly important for sensorineural hearing impairment where a medical diagnosis is difficult given the inaccessibility of the inner ear. Diagnosis in terms of pathology, e.g. outer hair cell (OHC) dysfunction, strial presbycusis, groups of unresponsive auditory nerve fibers, etc., is potentially more valuable than descriptive classifications based on the audiogram. Dubno and colleagues (2013) recently adopted a similar approach by describing audiometric phenotypes based on five hypothesized conditions of cochlear pathology.

A potential second benefit involves the practical use of an individualised model for tuning and optimizing hearing aids in the absence of the patient. This 'on the bench' approach also has the potential to compare the value of different types of hearing aid for a patient or even to develop new and better hearing aid algorithms. We call this the 'Hearing Dummy' technique by analogy with a tailor's dummy used to fit clothing to a customer's measurements without needing to have the customer present throughout the process. The development of such dummies requires two stages; 1) the initial psychophysical measurements and 2) the construction of the dummy itself. First, we measure the patient's hearing and then adjust a 'standard' computer model to suit. The criterion of success is that the adjusted model should yield the same hearing profile when measured using the

*same* testing procedures as those employed when assessing the patient. These principles are independent of the particular hearing tests used or the particular computer model that is used. The current paper is essentially an evaluation of the feasibility of the general approach. It uses a model that is familiar to the authors but it is not intended to claim that this is the only kind of model that could be used or, indeed, necessarily the best model.

Heinz et al (2001), Bruce et al (2003) and Zilany and Bruce (2006) modelled the consequences of damage to the auditory system for physiological measures in cats. They were able to evaluate the model performance by directly comparing model output and published physiological observations. Jepsen and Dau (2011), on the other hand used their model to simulate psychoacoustic data obtained from hearing-impaired individuals. Their results were related to contemporary attempts to make quantitative estimates of the auditory filter shapes and the amount of residual compression. The current study follows Jepsen and Dau in simulating psychoacoustic measurements but is more focussed on a global account of the pathology underlying the hearing problems of an individual. A preliminary account of this study was presented earlier (Meddis et al, 2010) and an extensive account is available in Panda (2010).

The psychoacoustic measurements used in this study include 1) absolute thresholds, 2) frequency selectivity and 3) compression; each measured using a range of probe frequencies. The development and assessment of the measurement procedures have been described elsewhere (Lecluyse et al, 2013; Tan et al, 2013). Their aim is to generate an auditory profile that summarises basic aspects of auditory functioning while also being simple enough to be used in the context of computer modelling. All three tests use a procedure where the listener is asked to say whether a probe tone (presented in silence) is audible or not. The computer model used in the current paper has been adapted to be able to deal with this simple psychophysical task. This has an important consequence. It means that the computer model can be tested using *exactly* the same procedure as used with the patient. The only difference is that the patient is tested in a sound-attenuated booth while the computer is electronically harnessed to the testing software.

Auditory models can have many parameters that determine various processes, and different configurations of these parameters may yield similar results. Hence, no solution is guaranteed to be unique. However, there are ways of ensuring that the final solution is reasonable. For example, a good model of the auditory periphery will normally be composed of a series of stages representing a cascade of physiological processes, each of which has been extensively studied in small mammals. This offers an opportunity to validate each stage of the model against published physiological measurements and this limits the scope for error. It also means that the parameters at each stage can be constrained to a range of physiologically meaningful values.

Another safeguard is created by requiring the model to fit a number of different measures for the same patient. Many different parameter sets might be used to simulate a simple audiogram. However, sets of successful parameters will be fewer when simulating frequency selectivity and compression measurements as well. Additional constraints can be added. For example, the current paper postulates that a particular pattern of hearing impairment may be caused by a pathological change affecting a single underlying physiological process. This means that a model has to simulate the difference between 'normal' hearing and a particular pattern of impairment by changing only a *single* parameter. This is a challenging requirement but the results indicate that it can sometimes be met.

It has also proved possible to make progress by assuming that the same parameter change applies at all locations along the cochlear partition. This is an even more severe constraint. Inspection of hearing impaired listeners' audiograms often shows deficits that vary with frequency. This leads to the intuition that parameters need to be set individually for each location in order to accommodate these effects. However, this may not always be the case. The constraint of a single pan-cochlear parameter change offers further validity to the choice of parameter and reassurance that a meaningful insight into the underlying pathology may be obtained. It is, of course, understood that this may not always be the case. For example, prolonged exposure to noise might affect many cochlear components (Feuerstein, 2002), rather than affecting only a single process. Nevertheless, it is instructive to study the effects of simple cases first.

This single parameter constraint is subject to one important caveat. It is often inferred from the audiogram or other tests that some parts of the system are unresponsive (so-called, ‘dead regions’). It is not always clear whether these arise from missing or dysfunctional inner hair cells, ineffective synapses, non-functioning spiral ganglion neurons or more central deficits. Where these regions can be inferred from the psychophysical test results, the model is first adjusted by disabling the auditory nerve fibers originating in the corresponding region of the cochlea. This step is taken before seeking to identify the critical parameter change that will transform a model of normal hearing into the impaired model.

The current paper will begin with a brief description of the data collection techniques. The computer model, which has already been described elsewhere (Meddis, 2006), will then be briefly introduced. A model for normal hearing will be compared with auditory profiles from normal listeners and then adapted to simulate different types of peripheral dysfunction. Finally, the application of the model will be illustrated by comparing the profiles it generates with those of the participants.

## **METHODS**

### ***1. Data collection***

#### **a. General principles**

The data collection procedure for measuring auditory profiles has been reported in previous studies (Lecluyse et al, 2013; and Tan et al, 2013) and is briefly outlined below. Three different psychophysical measurements were made; absolute thresholds, frequency selectivity and compression. In each case, the thresholds were estimated using a single-interval up/down (SIUD) procedure modified by Lecluyse and Meddis (2009) for rapid data acquisition in a clinical setting using volunteer patients. The same procedures were used for collection of the human auditory profiles and the computer model profiles, with only minor modifications for evaluating the models. Software for running these tests using MATLAB is available from the authors.

*Absolute thresholds.* Minimum detectable sound pressure levels were obtained for 8-ms and 500-ms pure tones at frequencies .25, .5, 1, 2, 4 and 8 kHz. In some cases, the 6-kHz threshold was also measured.

*Frequency selectivity* was assessed using a forward-masking paradigm, consisting of a 108-ms masking tone followed by an 8-ms probe tone presented at 10 dB above its own (8-ms) threshold. The gap between masker and probe was 10 ms. Within a run, the masker level was varied to determine the masking threshold for the probe. Between runs, the masker frequency was changed randomly across the following values, 0.5, 0.7, 0.9, 1, 1.1, 1.2, 1.3 and 1.6 times the probe frequency and resulted in an IsoForward Masking Contour (IFMC; Meddis et al, 2010; Lecluyse et al, 2013; and Tan et al, 2013). IFMCs were generated for probe frequencies .25, .5, 1, 2, 4, and 6 kHz.

*Compression* was also assessed using a forward-making task. Similar to the frequency selectivity measure, a 108-ms masking tone was followed by an 8-ms probe tone presented at 10 dB above its own (8-ms) threshold. Within a run, the masker level was varied to determine the masking threshold for the probe tone. Between runs, the gap between masker and probe was varied randomly and gaps used were 10, 20, 30, 40, 50, 60, 70, 80 and 90 ms. The resulting masker thresholds generated a Temporal Masking Curve (TMC). In all conditions, the masker frequency was identical to the probe frequency. TMCs were obtained for probe frequencies .25, .5, 1, 2, 4, and 6 kHz. The rationale for this procedure is that a compressed masker will need to rise more quickly to compensate for the increase in masker-probe interval. A loss of compression is indicated by a reduction in the slope of this function relative to the TMCs of listeners with normal hearing.

## **b. Stimuli**

Stimuli were generated using the MATLAB computer language and were presented through a computer sound card (Audiophile 2496, 24-bit, 96000-Hz sampling rate). All tones were pure tones, ramped with 4-ms raised-cosine onset and offset times (no steady-state portion for the 8-ms probes). All test stimuli were preceded by *cues* that were identical to the test stimuli but easier to hear. For example, the absolute threshold test consisted of a single target tone preceded by an identical tone that was 10 dB more intense. In the case of the procedures that used forward maskers (IFMCs and

TMCs), the cue was a masker-probe combination identical to the test stimulus except that the level of the masker was 10 dB lower, making the probe easier to hear. The time interval between the cue and test stimuli was 500 ms.

### **c. Threshold estimation procedure**

A cued, single-interval, up-down (SIUD) procedure (Lecluyse and Meddis, 2009) was used. A probe stimulus was presented to the participant who responded by indicating whether or not it was audible. The participant responded by means of a button box linked to a visual display. The level of the target was changed from trial to trial using a one-down, one-up adaptive procedure. For the *absolute threshold* task, if the participant responded positively (yes-response), the stimulus level was generally decreased by 2 dB. If the participant responded negatively (no-response), the level is increased by a 2 dB. A larger 10-dB stepsize was used up to the first reversal. For *IFMCs and TMCs* the level of the masker was *increased* following a positive response indicating that the target probe was heard and decreased following a negative response. The threshold was estimated using a best-fit logistic function relating level to the incidence of positive/negative responses.

There were ten trials in each run after the first reversal. Twenty percent of the trials were catch trials when no target was presented. Subjects were informed if they reported a target when none was present and the trial was restarted. Otherwise no feedback was given.

### **d. Task**

For human listeners, the 'yes-no' responses were not obtained directly. Instead, the listener was asked to count how many probe tones were heard; 0, 1 or 2. If the listener responded '2', it was inferred that both the cue and test probe had been heard and the response was scored as a 'yes'. If the response was '1' (only the easier cue-probe was heard) or a '0', it was scored as a negative response.

When evaluating the model, the cues were omitted and the model simply emitted a 'yes' or 'no' response. Model responses were based on the activity of a single 2<sup>nd</sup> order model brainstem neuron (see computer model section). If at least one action potential occurred during the presentation of the target probe tone, the emitted response was a 'yes' otherwise it was a 'no'.

### **e. Participants**

Data were collected from two participants with normal hearing (male, aged 29 and 21) and five participants with sensorineural hearing loss (2 female, 3 male, age range 50-77 years.). Normal hearing was determined by standard clinical measurements and thresholds better than 20 dB HL at all test frequencies. Sensorineural hearing loss was confirmed by using standard clinical audiometric tests (pure tone audiometry, tympanometry and acoustic reflex), thresholds were worse than 20 dB HL at one or more test frequencies. The participants with a hearing impairment were assessed as part of two larger studies (Lecluyse et al, 2013; Tan et al, 2013). The 5 impaired hearing data sets were selected with a view to illustrate different patterns of hearing loss. All listeners with a hearing impairment were regular users of hearing aids. The left ear was used in most cases; in one case the right ear was used.

## ***2. Computer Model***

The computer model of the auditory periphery used in this project was a slightly modified version of a previously published model (Meddis, 2006). The operation of the model can be divided into two stages. The first stage simulates the pattern of spike activity in the auditory nerve (AN). The second stage consists of a two-layer coincidence detection network based loosely on auditory brainstem circuitry. This network is designed to distinguish between spontaneous AN spikes and stimulus-driven activity. The threshold of the second and final layer of the network is set so that no spikes are emitted during silence. The output of this layer is monitored during the probe tone and, if any spikes are noted, the model is judged to have ‘heard’ the probe.

The equations for the model are given in full in Meddis (2006). The software to run the model are available from the authors.

The original model (Meddis, 2006) was modified in two respects. The first modification of the model concerns the dual resonance nonlinear (DRNL) filter that simulates the vibration of the basilar membrane (BM). Previously, the input to this module was stapes velocity but this has now been changed to stapes *displacement*. This minor change results in a substantial reduction in the number of parameters used to specify the DRNL filter. Previously, different gain parameters were required at

each location along the BM for both the linear and nonlinear pathways (see Meddis, 2006, Table I). The new arrangement requires only one gain parameter for each pathway irrespective of location. This simplification is not a change in substance but results from the fact that displacement itself varies as a function of frequency for a fixed sound pressure level. Our earlier practice of changing the gain parameter at each location was therefore an unfortunate consequence of our choice of input (velocity rather than displacement). Nevertheless, the new practice has important implications for describing individual hearing using a much smaller set of parameters.

The second modification concerns the coincidence network at the output of the model. Previously, this was modelled using a single model neuron per best-frequency (BF) channel. This was found to be unstable in forward-masking tasks (see the results in Meddis, 2006). Greater stability was obtained by establishing an extra layer of neurons. Now, each BF channel contains 10 1<sup>st</sup>-order neurons each receiving input from 10 AN fibers. All 10 of these neurons feed into a single 2<sup>nd</sup>-order neuron. The threshold of the 1<sup>st</sup>-order neuron is set to give a low spontaneous rate while the threshold of the 2<sup>nd</sup> order neuron is set to give no spontaneous activity at all. Consequently, any spikes in this neuron can be used to indicate that a stimulus is present and this is taken as a 'yes' response in the evaluations below. The 'yes' / 'no' quality of the output allows the model to be tested using the same software used to test human listeners and allows for a direct comparison in their answers.

The search for appropriate parameters to simulate the hearing impairment of an individual participant began with a 'standard' model designed to simulate the hearing profile of an individual with normal hearing. Parameter changes were then sought that would simulate a particular pattern of impairment. This search was guided by 'reasonable hypotheses' as to the likely pathology. The search was not exhaustive because of the large number of available parameters. While many possibilities were explored, it became clear that convincing profiles could be generated by changing only one parameter per participant.

A two-stage process was adopted when seeking appropriate parameters for the model. First, unresponsive regions were identified and channels with corresponding best frequencies (BFs) were simply deleted from the model. The second stage involved finding a *single* parameter change that

would convert the standard model to the impaired model. This restriction yielded fits to the data that were less than perfect but were close enough to suggest that the parameter change might represent the predominant pathology affecting the participant's hearing. The modelling procedure is based on the assumption that the participant's pre-morbid hearing was the same as that represented by the standard model which can, of course, be only an approximation. No attempt was made to manipulate multiple parameters in order to give a tight fit to the data.

One unsolved problem needs to be acknowledged. The patient profile IFMCs and TMCs were obtained routinely using a probe whose amplitude was fixed at 10 dB above the threshold for the probe. When running the model, it was frequently found that probes at this level required unrealistically high masker levels to obtain masked threshold. As a work-around when testing the model we used less intense probes (typically 4-8 dB above probe threshold). These were fixed for a given probe frequency but chosen to match the patient average masker levels. It is possible that the model is over-estimating the increase in threshold for the 8-ms probe relative to the absolute threshold for 500-ms tones and this is providing an inappropriate probe level for assessing the TMC. This could be a consequence of inappropriate temporal integration in the model but a definitive explanation cannot be given at this time.

The standard evaluation procedure used a 21-channel model with BFs equally spaced on a log scale between .25 and 8 kHz, except where explicitly specified. When an unresponsive region was identified on the basis of asymmetric IFMCs, channels in this region were deleted and an extra active channel was inserted into the model at the edge of the responsive region (or two extra channels if the dead region was bounded by two active regions).

## RESULTS

### 1. *Human auditory profiles*

#### a. **Normal-hearing data**

Fig. 1 (top panel, left column) shows the hearing profile of one normal-hearing listener (NH81). This visual display was presented and discussed in detail by Lecluyse et al (2013). The absolute thresholds for 500-ms tones are displayed at the bottom of the profile (expressed as dB SPL) connected by a line. All thresholds lie within normal limits. The V-shaped functions above the absolute thresholds show IFMCs at different probe frequencies (the unfilled circle indicates the masker level when the masker is at the same frequency as the probe). A narrow V-shaped function is an indicator of good frequency selectivity since masker thresholds at frequencies different from the probe frequency are considerably higher compared to the masker threshold at probe frequency. Immediately above each function is a numerical estimate of the ‘depth’ of the IFMC (in dB). The depth is defined as the difference between the average of masker levels at frequencies  $0.7^*$  probe frequency and  $1.3^*$  probe frequency and the masker level at the expected tip (i.e. at  $1^*$  probe frequency). This measure is large when the V-shape is narrow and symmetric. Any deviation from this pattern will reduce the depth.

TMCs are at the top of the profiles and the probe frequency is posted above each function. The TMC abscissa is the masker-probe gap and the ordinate is the masker level required to mask the probe for a given gap. Steep TMCs are taken to indicate good compression because the compressed masker needs to increase substantially to compensate for increases in the masker-probe time interval. A ‘slope’ estimate (in dB/100 ms) is posted immediately below each function. The ‘slope’ of the TMC is simply the slope of the least-squares best-fit straight line to the TMC thresholds. A large slope-measure is associated with a steep TMC.

A second, normal-hearing profile (NH83) is also shown in Fig. 1 (bottom panel, left column). These two profiles are typical of a number of other profiles of normal-hearing listeners (Tan et al,

2013). They typically show steep-sided, V-shaped IFMCs with their tips at the probe frequency and steep TMCs. This general pattern will be referred to below as ‘normal’.

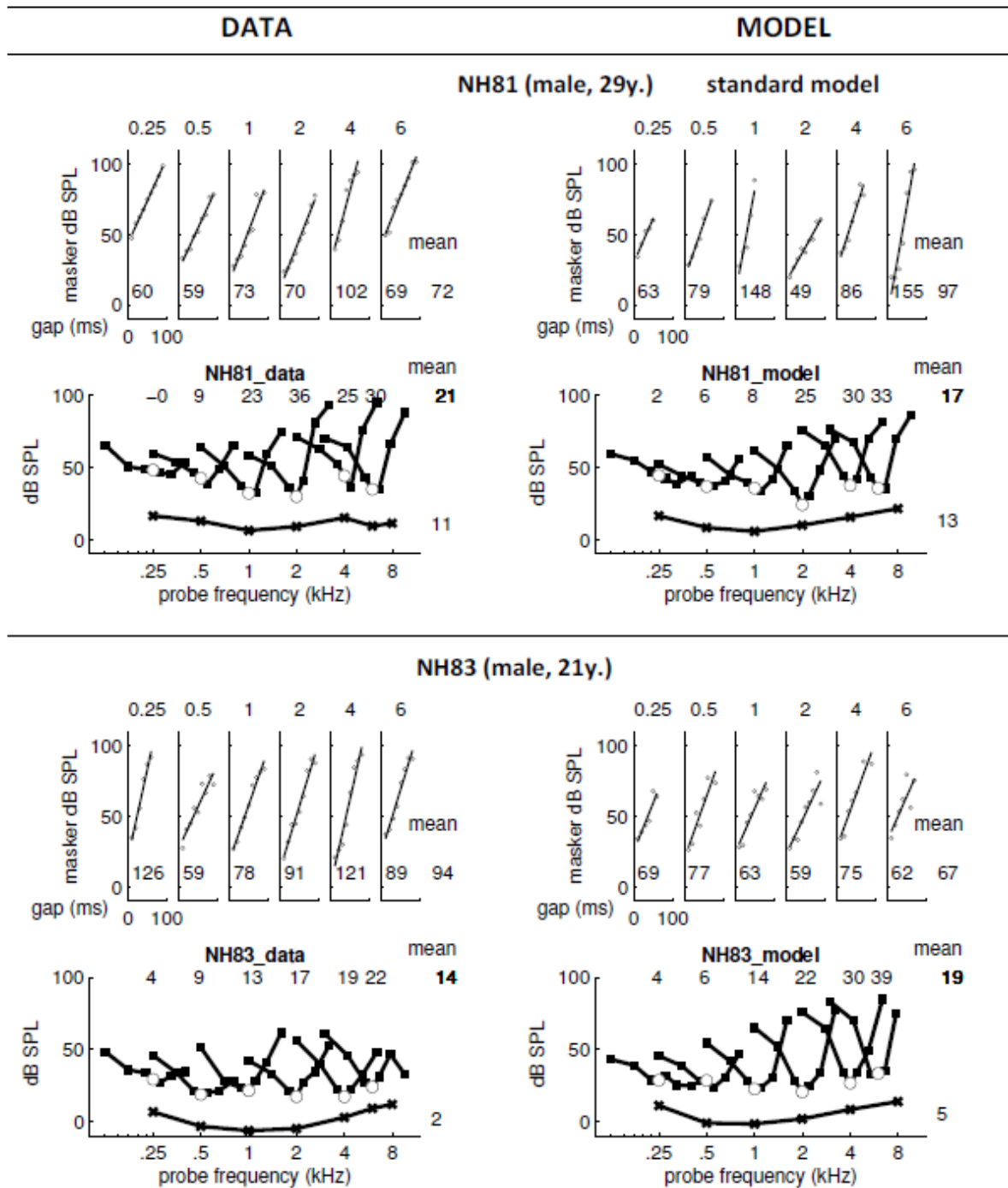


Fig. 1. Normal-hearing profiles. *Left column*: human auditory profiles for two listeners with normal hearing. *Right column*: computer model profiles of these normal hearing listeners. The computer model

for NH81 in the top right panel is the standard model used as the basis for creating all other models. TMCs are at the top of the profiles and the probe frequency is posted above each function. IFMCs are shown at the top of the lower figure. The unfilled circles indicate the masker level when the masker is at the same frequency as the probe. Absolute thresholds are at the bottom of the profile. The numbers in the body of the profile give the TMC slope estimates, and the IFMC depth estimates for each frequency. Values on the right hand side are mean estimates of absolute thresholds, IFMCS depth and TMC slope across all measured frequencies. For detailed information see in-text.

### **b. Impaired-hearing data**

Profiles for five listeners with impaired hearing are shown in the left column of Figures 2 and 3. *IH05* shows raised absolute thresholds at high frequencies, wider IFMCs than normal and only gently-sloping TMCs at all frequencies. *IH09* has a more profound loss with significantly raised absolute thresholds at low frequencies and no measurable thresholds at high-frequencies. IFMCs are abnormal, have no individual shape but follow the contour of the absolute threshold measurements. The TMCs have extremely shallow slopes<sup>1</sup>. *IH13* (Fig. 3) shows a steep high-frequency loss with IFMCs that are broader and TMCs that are shallower than normal. However the TMCs are distinctly steeper than *IH05* or *IH09*. *IH10* has a flat loss at the lower frequencies and gradual rising high-frequencies. The IFMCs are broader than normal, however the TMCs are almost as steep as normal hearing (except at the two highest frequencies measured). *IH07* has a mid-frequency hearing loss with IFMCs that are almost normal at 0.25 and 4 kHz but asymmetric at all other frequencies. TMC slopes are shallow.

---

<sup>1</sup> This almost horizontal function appeared to call into question the measurement technique. This is because forward masking was apparently independent of the duration of the gap between the masker and the probe. Supplementary tests with this subject were carried out using much longer gaps. It was found that the masker was indeed rising but very slowly as a function of gap duration. The same phenomenon has been observed in a small number of other patients. The data suggest a complete absence of compression so that a small rise in masker levels results in a considerable increase in forward masking. The phenomenon invites further research.

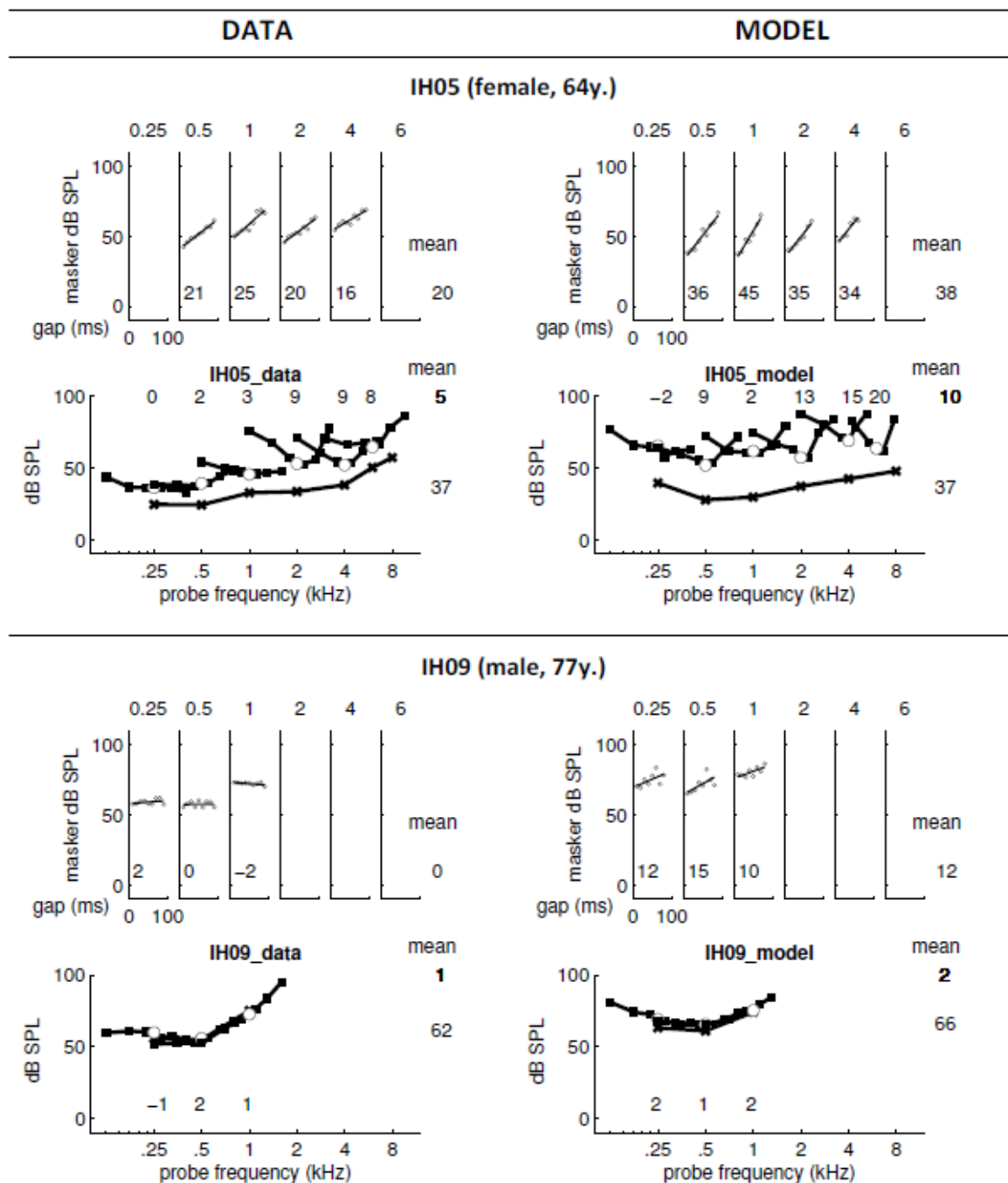


**Fig. 2. Impaired-hearing profiles.** *Left column:* human auditory profiles for two listeners with impaired hearing. The format of the individual profiles is the same as Fig. 1. Missing data at high frequencies indicate that measurements could not be made because of the hearing loss. Missing data at low frequencies indicate that the data were not collected for some practical reason. *Right column:* computer model profiles of these impaired listeners. The parameter changes required to create the model profiles are shown in the text.

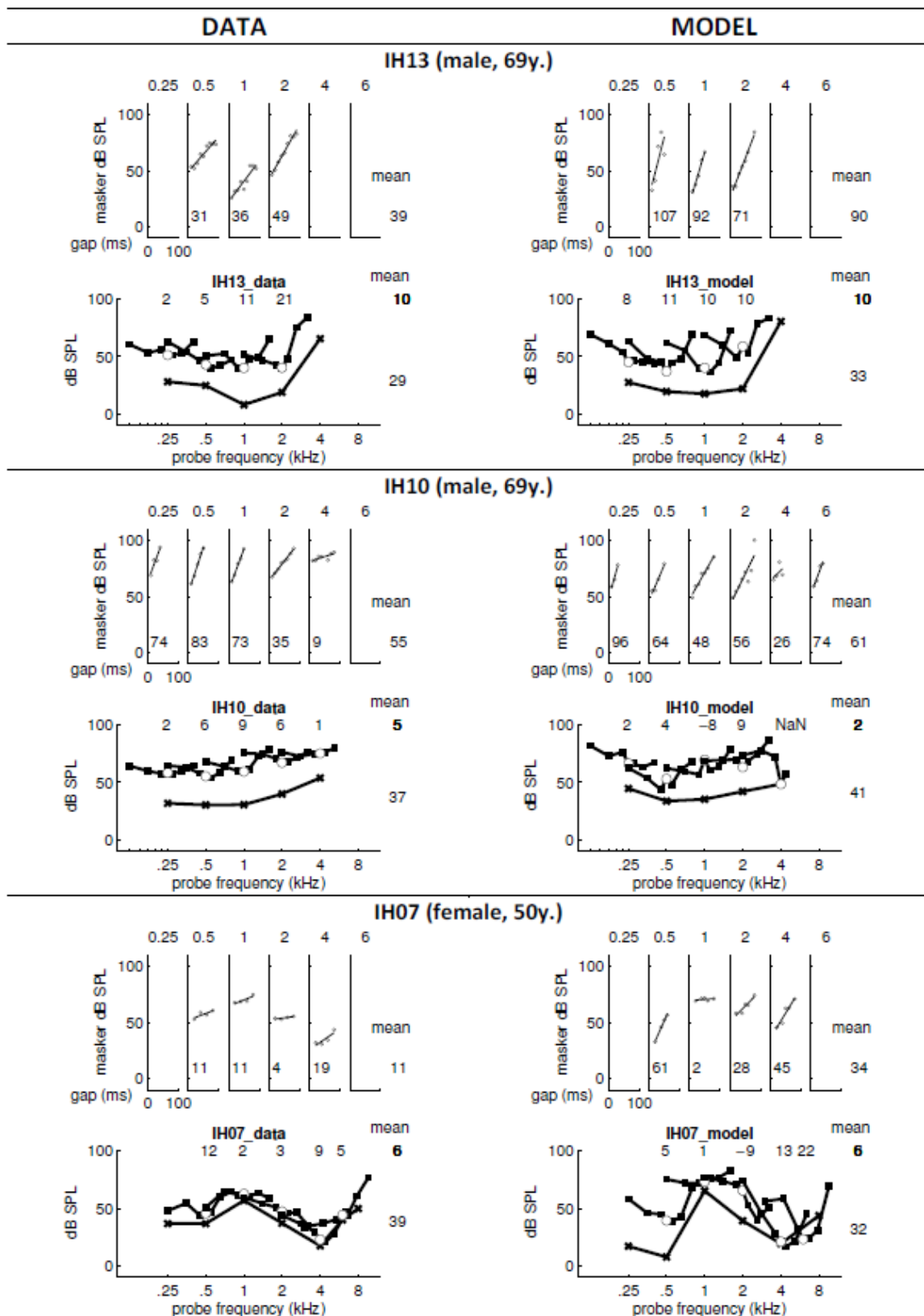


Fig. 3. Same as Fig. 2. *Left column*: human auditory profiles for three listeners with impaired hearing. *Right column*: computer model profiles of these impaired listeners.

## 2. Computer modelling results

### a. Models of normal hearing

The data from NH81 was used to create a model of normal hearing (Fig. 1, top right). The choice was arbitrary given that either of the two normal-hearing profiles could have been used. This model of normal hearing will be referred to as the ‘standard model’ because it was used throughout as the baseline for all further explorations. The parameters for this model are given in Appendix A in Table A1.

The difference between the 2 normal-hearing profiles was explored by searching for a fit to the data generated by participant NH83. A small increase in the nonlinear gain of the DRNL module was enough to provide an adequate fit to the data of NH83. This gain parameter (DRNL.a) is a scalar that converts stapes displacement to BM displacement and represents the contribution of OHCs. This gain factor is effective at levels below the level at which the response becomes compressed. In this example, the factor was increased from  $1.2 \cdot 10^6$  to  $2.0 \cdot 10^7$ . Absolute thresholds are lowered as a consequence of the increased gain while other features of the profile remain unchanged. Note that, in the adjusted version of the model, the same DRNL gain is used at *all* locations along the cochlear partition. Consequently, a single parameter change reduces thresholds at all probe frequencies.

### b. Models of impaired hearing

*IH05.* A model of IH05’s mild hearing loss was obtained by decreasing the gain of the DRNL filter in the standard model by *reducing* the DRNL.a parameter from  $1.2 \cdot 10^6$  to  $5 \cdot 10^4$ . The resulting profile is shown in Fig. 2 (top, right panel). The model absolute thresholds are raised compared to the standard model (Fig. 1, top right panel) at all frequencies because the same value of DRNL.a is used at all BFs.

This single parameter change produces two other effects: the IFMCs are broader and the TMCs are less steep than for the standard model. The explanation for this combination of three different effects from a single parameter change can be found in the architecture of the DRNL filter used to represent

the mechanical response of the cochlear partition (Lopez-Poveda and Meddis, 2001). Its output is the sum of two processes, one linear and the other compressively nonlinear. For low to moderate levels, the nonlinear path has a higher gain than the linear path and is more narrowly tuned. The DRNL.a parameter applies only to the *nonlinear* path. When the nonlinear gain parameter is reduced, the relative contribution of the nonlinear path is reduced and the output of the more broadly-tuned linear path comes to dominate the output producing wider IFMCs. Wider IFMCs were also found in normal-hearing listeners, when tested with high probe levels (Tan et al, 2013). Modelled TMCs are shallower because the response to the masker is now less compressed and, as a consequence, a smaller increase in the masker is required to compensate for increases in the masker-probe gap.

The model and patient profiles are discrepant at 250 Hz. This could not be remedied without violating our single-parameter change restriction. The standard model has a rise in threshold at 250 Hz and the impaired model reflects this normal pattern when the gain reduction is applied by reducing the DRNL.a parameter equally at all frequencies. Clearly, it would be possible to improve the fit by making an *ad hoc* adjustment to the gain at this frequency. However, there may be other explanations and we have left the matter open.

*IH09.* A model that gives a useful fit to IH09's profile was created by defining all locations of the standard model's cochlea as unresponsive *except* for an island of activity at 250 Hz modelled as a *single* surviving channel (Fig. 2, bottom, right panel). The nonlinear pathway in the DRNL filter in this one remaining channel was also disabled by setting its gain parameter to zero. Only the linear pathway of this channel was left intact. The absence of any compression resulted in shallow TMCs. When there is no compression, a small increase in masker level is enough to compensate for the increase in the time interval between masker and probe. The 250-Hz absolute threshold is now determined by the gain in the linear pathway alone, which was left unchanged (parameter DRNL.g). The high thresholds at the other probe frequencies are explained by the necessity to detect all sounds through this single remaining channel. The absolute thresholds at each frequency simply reflect the tuning of the 250-Hz channel.

The IFMCs at all probe frequencies follow the contour of the 250-Hz IFMC so closely that they are difficult to distinguish from the absolute thresholds. Consequently, the IFMCs at frequencies other than 250 Hz are asymmetric about their probe frequencies. This asymmetry was the original indication that there was only one active channel.

*IH13*. The third impaired-hearing profile (Fig. 3, top row, right panel) was modelled using a combination of reduced DRNL gain after first eliminating a number of channels in a 'dead region'. The absolute thresholds for this individual rise steeply above 2 kHz and the IFMCs in this region are asymmetric. This was taken to indicate that all channels above BF= 1750 Hz are unresponsive. To model this, all channels in the standard model with BFs = 2 kHz and above were disabled and a new channel was added at 1750 Hz. This additional channel was needed to represent the limit of the active region. It is assumed that it is used to detect all pure tones above this frequency. The dead region was inferred based on an extremely high threshold at 4 kHz and an asymmetric IFMC at 2-kHz indicating off-frequency listening (similar as in Moore and Alcantara, 2001). Thresholds in the active frequency region (below 1750 Hz) are also raised and this was taken to indicate reduced gain in the nonlinear path. The nonlinear response in all active channels was therefore attenuated by reducing the DRNL.a parameter from  $1.2 \times 10^6$  to  $3.0 \times 10^4$ . The model TMCs for IH13 are similar to those in the standard model profile. This is because the compressive nonlinear pathways continue to be active in the remaining channels.

*IH10* (Fig. 3, middle row, right hand panel). So far, all impaired models have been produced by a combination of channel deletion and a reduction in the gain of the nonlinear pathway of the DRNL filter in the remaining channels. However, this strategy does not work for profiles with a flat loss at lower frequencies and a gradual high-frequency slope because channel deletion at all high frequencies produces steep threshold slopes above the deleted channel (see the modelled profile of IH13). In this respect, the profile for IH10 presents an interesting challenge. Furthermore, the TMCs of IH10 are almost as steep as normal TMCs indicating residual compression. This profile could not be modelled simply by changing the DRNL.a parameter.

These profile features suggested a dysfunction of the inner hair (IHC) cell system. Strial presbycusis is characterised by a reduced endocochlear potential (EP) consequent upon atrophy of potassium-secreting strial cells in the lateral wall of the scala tympani. This type of presbycusis can result in hearing loss across all frequencies but the loss is greatest at high frequencies (Schuknecht and Gacek, 1993; Schmiedt *et al*, 2002). Schmiedt *et al* (2002) also found that otoacoustic emissions remain 'robust' when the EP is artificially reduced by application of furosemide, suggesting that the reduction in EP has a greater effect on IHC than OHC functioning. Given that IHCs and OHCs are both driven by the EP one might expect that a reduction in the standing potential would affect both equally but this is not the case. Mills *et al* (1993) found that a reduction in distortion product otoacoustic emissions (DPOAEs) did occur alongside artificial reduction of EP, but only after large reductions in EP and only for a relatively short period of time (around 30 min.). They demonstrated that DPOAEs quickly return to normal even when the EP reduction is sustained. Consequently, a dissociation of IHC and OHC function is likely when the EP is chronically reduced.

The impaired model was created using the standard model with a single parameter change, a reduction in the EP from 120 mV to 87 mV. This is a variable in the IHC computer simulation representing the voltage difference across the cuticular plate. It is a global variable that applies to IHC components at all BFs but does not affect DRNL function. The resulting profile is shown in Fig. 3 (middle row, right panel). Absolute thresholds are raised with a steeper increase at high frequencies. The IFMCs are broader and this is consistent with the need to make measurements at higher signal levels (see the explanation given for the same outcome for IH05 above). The TMCs retain a near-normal slope indicating that compression is largely unaffected by this procedure. Because probe thresholds are higher than normal, the TMCs begin at an elevated level and rise rapidly to the maximum values allowed by the testing system (100 dB SPL).

The greater increase in absolute thresholds for this model at higher frequencies is an emergent property of the model. Some insight into the effect can be gained by inspection of Fig. 4 that shows the model auditory nerve (AN) rate/ level function at two frequencies (500 and 4000 Hz) and at two EPs (-120 and -87 mV). The fall in receptor potential that accompanies the reduction in EP is the

same at high and low frequencies, i.e. the functions are displaced identically downwards. However, threshold is exceeded when receptor potential exceeds some critical value (here set at  $-42$  mV). It can be seen that the level at which the function crosses the threshold line increases more for the high-frequency tone. This is a consequence of the difference in slope of the receptor potential functions in Figure 4. Of course, threshold is not simply determined by receptor potential but by coincidence detection and this simplified example is for illustrative purposes only.

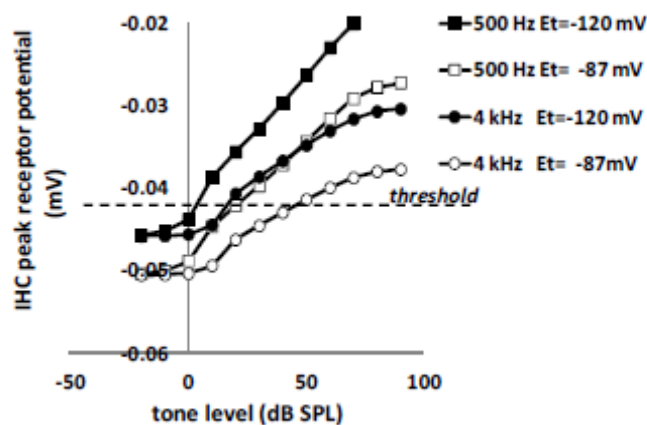


**Fig. 4: Illustration of how EP reductions affect the thresholds for high frequencies more than low frequencies. The chart shows model inner hair cell peak receptor potential as a function of sound level for a low- and a high-frequency sinusoidal stimuli at a range of tone levels for two values of EP ( $-120$  mV and  $-87$  mV). The dashed horizontal line indicates a threshold voltage that needs to be exceeded in order to generate coincidence detection in subsequent model stages. When EP is reduced, the 500 Hz and 4 kHz functions shift down by the same amount but the threshold crossing point is shifted more to the right for the 4 kHz tone suggesting a greater rise in threshold at this frequency.**

*IH07*. The profile of *IH07* (Fig. 3, bottom row, right hand panel) is that of a mid-frequency hearing loss indicating a clear dysfunction in a frequency region between 1 and 2 kHz. At lower frequencies there is a region of reduced residual function. At higher frequencies above 2 kHz an island of near normal functioning appears to be operating. The model hypothesises two islands of active channels 1) between 250 and 360 Hz and 2) between 3000 and 4400 Hz. All other channels were deleted and new

channels created at the borders of the active regions. The reduced list of BFs used in the model was .25, .46, 2.7, 4.4 and 6.2 kHz. The model, therefore, attempts to explain the patient's impaired hearing simply in terms of two isolated regions of preserved hearing. It will be shown to be an oversimplification and, as a result, the model profile is not perfect. Nevertheless, it still serves to illustrate some useful principles concerning how to understand the origin of the observations made in the middle of the unresponsive region. For example, the raised absolute thresholds at 1 kHz must be understood in terms of processing taking place in adjacent regions. One or the other region (or both) must be contributing to the detection of the probe.

Similarly, the IFMCs must also reflect processing in the remaining functional channels. Symmetric, V-shaped IFMCs can be seen in both model and human profiles at 500 Hz and 4 kHz. In the model and possibly the patient this reflects residual hearing at these frequencies. If so, the patient's approximately flat IFMC at 1 kHz must be explained in terms of the combined effect of processing taking place in these remote high- and low-frequency regions. If the probe is at 1 kHz and the masker is at a lower frequency then detection of the probe is more likely to take place at the *higher* 2.7-kHz filter where the masker is less effective. The opposite is true for lower frequency maskers. The model predicts an IFMC that is approximately flat. It is not a perfect fit to the patient's data but hints at how an unresponsive region can nevertheless yield an approximately flat TMC at its centre.

A different picture emerges for IFMC tests using the 2-kHz probe. On this occasion, the nearest functioning filter in the model (2.7 kHz) is much closer to the probe frequency than the highest functioning low-frequency filter (0.46 kHz). As a consequence, the IFMC for the 2-kHz probe will reflect, almost exclusively, the response of the 2.7 kHz filter so that the masker will be more and more effective the closer it is in frequency to 2.7 kHz. The model predicts a diagonal function which is qualitatively similar to the patient data..

IH07's TMCs are all shallow and this indicates an absence of compression in the residual responsive regions. This is not represented well in the model. As a result, the TMCs are unrealistically steep in the model profile and the absolute threshold for 0.25- and 0.5-kHz probes are unrealistically

low. This difficulty might have been circumvented by reducing the DRNL.a parameter in this region. However, a different value of DRNL.a would be required in the high-frequency regions, particularly at 4.4 kHz to account for the almost normal absolute threshold at 4 kHz. All of these changes would result in a violation of our rule of using only a single parameter change to represent a single underlying pathology. This leaves us with a profile that illustrates how unresponsive regions can determine the shape of the auditory profile but also a reminder that not all examples of impairment respond readily to the principles embodied in the particular model used in this study.

## DISCUSSION

The current paper showed that it was possible to generate individualised computer models of the impaired hearing of specific individuals and to evaluate each model against the patient data using the same data acquisition procedures for both patient and model. From a scientific point of view, the models represent hypotheses concerning the pathology that gives rise to the hearing deficit. These hypotheses could, in principle, be validated or invalidated using further measurements involving a wider range of techniques. From a clinical point of view, the model offers a way of identifying the pathological basis of the impairment and interpreting it to the patient. It also has promise as a tool for tuning prostheses and evaluating the suitability of competing hearing aid designs with respect to a particular patient.

The ability to compare the model performance against human psychophysical measures obtained using the same testing procedures is a novel development and distinguishes this study from other recent efforts to model hearing impairment (Heinz et al, 2001; Bruce et al, 2003; Zilany and Bruce, 2006, Jepsen and Dau, 2011; Meddis et al, 2010) although all of these models could, in principle be adapted for this purpose. However, the current model is limited to this simple tone-in-silence test and future efforts need to be directed to extending the model's range to the more difficult issue of modelling the detection of tones in a simultaneous masking noise.

An individualised model is essentially a hypothesis concerning the possible pathology affecting a patient's hearing. The models in this paper hypothesise three different pathologies; unresponsive

regions, dysfunction of the BM mechanical response and reduction of EP. Nevertheless, it is not possible to offer any guarantee that these are the only hypotheses to give a good account of the patient data. Moreover, computer models of the auditory periphery, despite their complexity, fall well short of the complexity of the cochlea itself. There are other processes such as the acoustic reflex and the olivo-cochlear efferent system that are missing. Recent modelling studies suggest that these processes may play an important role for speech recognition in noisy environments (Brown et al, 2010; Clark et al, 2012). Until these additional processes are incorporated, a focus on detailed parameterisation of models may be premature.

The self-imposed constraint of using only one pathology per patient (plus unresponsive regions) may seem to be over-restrictive but it has the merit of forcing the modeller to look for the simplest possible explanation. When many parameters are allowed to vary, the modeller is open to the accusation that any model can be made to fit any data with enough degrees of freedom. This accusation must be avoided. However, it is clear from the examples above that a relaxation of the restriction could have led to better fits to the patient data. This option was not exercised because of the merit of keeping the exposition simple. If more than one parameter was in play, the reader would have difficulty in appreciating how individual parameters influence the modelling outcome. Nevertheless, it is clear that, in practice better fits are possible than those presented here without stretching credulity too far.

A consensus is emerging in the literature that an age-related, gradually sloping high-frequency loss, is often associated with atrophy of the stria vascularis (Schuknecht, 1964; Schuknecht and Gacek, 1993, Schmiedt et al, 2002, Dubno et al, 2013) leading to a reduction of EP and a consequent reduction in auditory nerve activity. The modelling described above was explicitly guided by this hypothesis. However, a choice had to be made between OHCs and IHCs as the intermediate structures in this process. Schmiedt et al (2002) and Dubno et al (2013) identify the sloping loss as a consequence of a reduction in the 'cochlear amplifier', presumably through dysfunction of the OHCs. Unfortunately this appears to be in contradiction of the evidence. For example, Schmiedt et al (2013) themselves report that experimentally induced reductions in EP leave DPOAEs largely intact, tuning

largely unaffected and two-tone suppression functioning normally. Mills et al (1993) found that acute reductions in EP did reduce DPOAEs in the short term but this recovered within a short period of time even while the EP continued at a low level, suggesting that OHCs are able to adapt to these adversely low potentials. For this reasons, it was felt more appropriate to explore the consequences of reduced EP on IHC functioning.

In the model, a reduction in EP applied exclusively to the IHCs resulted in raised thresholds in the form of a gradual increase in thresholds with frequency. This result was not anticipated and was difficult, at first, to understand. This is why a detailed explanation of the effect is given above. Of course, a model demonstration does not decide the IHC/OHC issue one way or another. This will depend on further empirical observations. However, the model does predict that a reduction of EP could lead to a sloping high-frequency loss solely through its effect on IHCs. An attractive feature of the prediction is that the same EP reduction at all places in the cochlea will give gradually rising thresholds with frequency. On the other hand, explanations based on OHCs (and hence the cochlear amplifier) require that the EP reduction be matched to the rise in threshold at each location. Alternatively, it requires gradually increasing sensitivity to EP reduction between the base and the apex.

The broader tuning observed in elderly, gradual sloping loss, patients may, at first sight, contradict the account based on IHC dysfunction. However, this is not the case. When a patient has raised thresholds, assessments of tuning must necessarily be made at higher signal levels. Even normal listeners show broader tuning when more intense probes are used. Tan et al (2013) used the same measurement procedures as those described above and found broader tuning curves (IFMCs) in normal-hearing listeners when higher probe levels were used. Moreover, the IFMCs of normal listeners obtained using more intense probes were comparable in width to the IFMCs of patients with gradually sloping high-frequency losses tested at the same levels. Reduced frequency selectivity in these cases cannot therefore be used as evidence of OHC dysfunction. In the same study, Tan et al (2013) found that many tinnitus sufferers had gradually sloping high frequency losses and these were

typically associated with indications of residual compression. Again, this makes an explanation in terms of OHC dysfunction less likely than one based on reduced sensitivity of IHCs.

The modelling efforts described above were constrained by the desire to describe individual hearing impairments in terms of three common pathologies; unresponsive regions, OHC dysfunction and loss of EP. In the interest of seeking the simplest possible explanation, it has been assumed in the models that reductions in OHC gain and loss of endocochlear potential were the *same at all points along the cochlea*. This is a novel assumption because it is often assumed that a raised threshold must indicate a reduced OHC gain at the corresponding frequency. Nevertheless, it was decided to evaluate the simplest possible assumptions first and the model results suggest that it might not be necessary to make separate OHC gain changes along the cochlea to get a range of different threshold patterns. There are two reasons for this outcome. First, unresponsive regions can explain steep slopes in the audiogram even though these may not involve OHC dysfunction. Second, endocochlear potential changes can explain gradual sloping high frequency losses.

Individualised computer models of a patient's hearing have the potential to enhance understanding of the problems faced by a particular patient in terms of an underlying pathology, particularly for sensorineural impairment where physical indications are difficult to identify. The principle is a general one and is neither restricted to the particular model used here, nor to the particular methods for assessing hearing. As computer models become more sophisticated and as assessment methods improve, it may be possible to generate individualised 'hearing dummies' whose usefulness extends beyond understanding a patient's problem to contribute to the development of improved and targeted prosthetic strategies.

## Acknowledgements

The authors would like to thank the participants for donating time and effort to the study and the associate editor Jacek Smurzynski and two anonymous reviewers for their helpful comments and suggestions on this manuscript. This research was supported by EPSRC, Deafness Research UK and DFG JU 2858/1-1.

## References

Brown, G.J., Ferry, R.T. and Meddis, R. 2010. A computer model of auditory efferent suppression: implications for the recognition of speech in noise. *J Acoust Soc Am* 127, 943-954.

Bruce, I.C., Sachs, M.B., and Young, E.D. 2003. An auditory-periphery model of the effects of acoustic trauma on auditory nerve responses. *J Acoust Soc Am* 113, 369-388.

Clark, N.R., Brown, G., Jürgens, T. and Meddis, R. 2012. A frequency-selective feedback model of auditory efferent suppression and its implications for the recognition of speech in noise. *J Acoust Soc Am* 123, 1535–1541.

Dubno, J.R., Eckert, M.A., Lee, F.S., Matthews, L.J., and Schmiedt, R.A. 2013. Classifying human audiometric phenotypes of age-related hearing loss from animal models. *J Assoc Res Otolaryngol* 14, 687-701.

Feuerstein, J.F. 2002. Occupational Hearing Conservation. Katz, J. (Ed) *Handbook of Clinical Audiology*. Baltimore: Lippincott Williams & Wilkins.

Heinz, M.G., Zhang, X., Bruce, I.C., and Carney, L.H. 2001. Auditory nerve model for predicting performance limits of normal and impaired listeners. *Acoustics Research Letters Online* 2, 91-96.

Jepsen, M.L., and Dau T., 2011. Characterizing auditory processing and perception in individual listeners with sensorineural hearing loss. *J Acoust Soc Am* 129, 262-281.

Lecluyse, W., and Meddis, R. 2009. A simple single-interval adaptive procedure for estimating thresholds in normal and impaired listeners. *J Acoust Soc Am* 126, 2570-2579.

Lecluyse, W., Tan, C.M., McFerran, D. and Meddis, R. 2013. Acquisition of auditory profiles for good and impaired hearing. *Int J Audiol* 52, 596-605.

Lopez-Poveda, E.A., and Meddis, R. 2001. A human nonlinear cochlear filterbank. *J Acoust Soc Am* 110, 3107-3118.

Meddis, R. 2006. Auditory-nerve first-spike latency and auditory absolute threshold: a computer model. *J Acoust Soc Am* 119, 406-417.

Meddis, R., Lecluyse, W., Tan, C.W. and Panda, M.R., and Ferry, R.T. 2010. Beyond the audiogram: Identifying and modeling patterns of hearing deficits. Lopez-Poveda, E.A., Palmer, A.R.,

and Meddis, R. (Eds.). *The neurophysiological bases of auditory perception*. Springer: New York, pp. 631-640.

Mills, D.M., Norton, S.J. and Rubel, E.W. 1993. Vulnerability and adaptation of distortion product otoacoustic emissions to endocochlear potential variation. *J Acoust Soc Am* 94, 2108-2122.

Moore, B.C.J. and Alcántara J.I. 2001. The use of psychophysical tuning curves to explore dead regions in the cochlea. *Ear Hear* 22, 268-278.

Panda, M.R. 2010. *Computer Models of Normal and Impaired Hearing*. PhD thesis, University of Essex, UK.

Ruggero, M.A., and Rich, N.C. 1991. Furosemide alters organ of corti mechanics: evidence for feedback of outer hair cells upon the basilar membrane. *J Neurosci* 11, 1057-1067.

Schmiedt, R.A., Lang, H., Okamura, H.O., and Schulte, B.A. 2002. Effects of furosemide applied chronically to the round window: a model of metabolic presbycusis. *J Neurosci* 22, 9643-9650.

Schuknecht, H.F. 1964. Further Observations on the Pathology of Presbycusis. *Arch Otolaryngol* 80, 369-382.

Schuknecht, H.F. and Gacek, M.R. 1993. Cochlear Pathology in Presbycusis. *Acta Oto Rhinol Laryngol*, 102, 1-16.

Tan, C.M., Lecluyse, W., McFerran, D., and Meddis, R. 2013. Tinnitus Patterns and Hearing Loss. *J Assoc Res Otolaryngol*, 14, 275-282.

Zilany, M.S.A. and Bruce, I.C. 2006. Modeling auditory-nerve responses for high sound pressure levels in the normal and impaired auditory periphery. *J Acoust Soc Am*, 120, 1446–1466.

## Appendix A

Table A1. Parameters for the computer model of the normal auditory periphery chosen to fit the data for NH81.

These should be read in conjunction with the equations given in Meddis (2006).

OME	air -> stapes displacement (scalar) high-pass cut-off frequency (Hz) filter order	1e-7 1300 2
DRNL	<i>a</i> gain <i>b</i> gain <i>c</i> compression exponent <i>p</i> for computing <i>n</i> l <i>BW</i> <i>q</i> for computing <i>n</i> l <i>BW</i> <i>g</i> linear gain <i>linBW</i> (Hz) varies with BF <i>Order of all gammatone filters</i>	1.2e8 2e-2 0.2 2.5e-4 1.4 5e5 <i>BF/3</i> 3
IHC Cilia	$\tau_c$ cilia/BM time constant (s) $g_{cilia}$ , cilia/BM coupling gain $G_{cilia}^{max}$ , max. conductance (S) $G_0$ , resting conductance (S) $s_0$ , displacement sensitivity ( $m^{-1}$ ) $u_0$ , displacement offset (m) $s_1$ , displacement sensitivity ( $m^{-1}$ ) $u_1$ , displacement offset (m)	3e-4 60 8e-9 2.7e-9 5e-3 0 5e-3 0
IHC	$E_i$ , endocochlear potential (V) $E_k$ , potassium reversal potential (V) $R_p/(R_i+R_p)$ , correction factor $C_m$ , total capacitance (F)	120e-3 -80.5e-3 0.1 16e-12
IHC/ AN	$E_{Ca}$ , reversal potential (V) $\beta_{Ca}$ $\gamma_{Ca}$ $\tau_m$ membrane (s) $\tau_{Ca}$ , calcium clearance (s) HSR LSR $z$ , $[Ca^{2+}]^3$ to probability scalar $G_{Ca}$ max, $Ca^{2+}$ conductance	0.066 400 130 1e-4 150e-6 550e-6 2e42 16e-9
AN	$y$ , replenishment rate ( $s^{-1}$ ) $l$ , loss rate ( $s^{-1}$ ) $x$ , reprocessing rate ( $s^{-1}$ ) $r$ , recovery rate ( $s^{-1}$ ) $M$ , maximum free transmitter quanta	3 2580 30 6580 12
MacG (CN)	$f_d$ , Dendritic low-pass cutoff (Hz) $\tau_m$ , membrane time constant (s) $C_m$ , membrane capacitance (Farad) $\tau_{Gk}$ , K+ recovery time constant (s) $b$ , increment in $G_k$ after spike (S)	50 2e-3 16.7e-9 2e-3 133e-6

	$Th_0$ , threshold (V)	10e-3
	$E_k$ K+ reversal pot. (V re resting)	-10e-3
MacG (IC)	$f_d$ , Dendritic low-pas cutoff (Hz)	100
	$\tau_m$ , membrane time constant (s)	0.5e-3
	$C_m$ , membrane capacitance (Farad)	16.7e-9
	$\tau_{Gk}$ , K+ recovery time constant (s)	1e-3
	$b$ , increment in $G_k$ after spike (S)	133e-6
	$Th_0$ , resting threshold (V)	10e-3
	$E_k$ K+ reversal pot.l (V re resting)	-10e-3